Electronic and magnetic structure of $Sr_2Fe_3S_2O_3$: a 2-D AFM spin ladder system

Dilruba Khanam[1], Asif Iqbal[1], and Badiur Rahaman[1]*

[1]Aliah University, IIA/27-Newtown, Kolkata-700156, India

Email: badiur.rahaman@gmail.com

Abstract

Electronic structure calculation has been carried out for quantum spin system $Sr_2Fe_3S_2O_3$ with an aim to figure out the underlying spin model. We present first-principles density functional calculation to study the electronic and magnetic properties of $Sr_2Fe_3S_2O_3$. We discuss explicitly the nature of the exchange paths and provide quantitative estimates of magnetic exchange couplings. A microscopic modelling based on analysis of the electronic structure of this system puts it in the interesting class of 2-D antiferromagnetic spin S=2 ladder system.

Keywords: Spin ladder system, Electronic structure, Magnetic exchange interactions, Spin model.

1. Introduction

Low dimensional quantum spin systems offer rich physics due to dominance of the quantum fluctuation in the low energy regime. Quasi-one-dimensional and quasi-two-dimensional spin-1/2 or spin-1systems,like odd- and even-leg ladders [1,2], quantum tubes [3], kagome, honeycomb and triangular layers [4–6] have received continuous attention due to enhanced importance of quantum effect stemming from reduced dimensionality and smallness of spin values. Bethe [7] showed that the quantum fluctuation prevent true long-range antiferromagnetic (AFM) order for homogeneous one dimensional (1-D) spin systems. In these systems the spin-spin correlation as a function of distance decays slowly to zero as power law. For two dimensional (2-D) spin systems, the Heisenberg model has a ground state with long-range AFM order only at T=0 K. Neither system has a spin gap, i.e., there is no cost in energy to create an excitation with S=1.The quantum fluctuation brings a dramatic effect in behaviour of compounds intermediate between 1-D and 2-D, i.e., quasi 1-D spin systems.These systems may have a finite energy gap between singlet ground state (S=0) and triplet excited state (S=1). The even-leg ladders [8], alternating Heisenberg antiferromagnetic chains [9], dimer systems[10], spin- Peierls systems [11] show gap in their spin excitation spectrum. Haldane [9] conjectured that a simple one dimensional magnetic chain would have a spin gap for all integer spins, but would be gapless for half-integer spins, a conjecture that has been backed up with considerable experimental evidence [12]. An analogous situation has been found to exist in the quasi-one dimensional spin ladder configuration, in which ladders with an even number of legs would exhibit an energy gap,but ladders with an odd number of legs would not [13]. Both the magneticsystems, dimers and alternating chains are one dimensional, while a ladder system is intermediate between a one and two dimensional system, called quasi1-D system. Therefore a ladder consists of two or more spin chains coupled together across“rung”.This additional coupling changes the character of the interaction from one dimensional to two dimensional. Classical spin-ladder compounds

gained considerable research attention now a days. Here are some examples of spin ladder compounds. For quantum spin, S=1/2 the ladder compound is $Sr_xCa_{14-x}Cu_{24}O_{41}$ (x = 0.4) [14], S=1 spin is found in the ladder compound $Na_2Ni_2(C_2O_4)_2(H_2O)_2$ [15]. For S=3/2 a noble ladder compound $Sr_2Co_3S_2O_3$ was discovered recently [16]. Now we discuss in this paper S=2 spin ladder compound $Sr_2Fe_3S_2O_3$ [17]. The ladder compound $BaMn_2O_3$ has S=5/2 spin [18].

In this paper we have studied the compound $Sr^2Fe^3S^2O^3$ with spin ladder crystal structure [19, 20]. There are two inequivalent Fe^{2+} magnetic sites are present in the compound. In our study we can clearly distinguish two sites and calculate their magnetic moments separately. To find the interaction in $Sr^2Fe^3S^2O^3$, we present the local density approximation (GGA) electronic structure of the compound and, starting from such description, we derive the total energy calculations of different spin configurations using VASP and we present the quantitative estimates of the dominant exchange interactions and infer the possible spin-model based on those estimates. The underlying spin model turned out to be rather interesting in several ways. Firstly, we find the exchange along the rung of the 2-leg ladder (SL) which is much more stronger than for necklace ladder (NL). Secondly, the Fe-Fe exchanges are found to be differing in sign, resulting into a spin-ladder with both AFM and FM exchanges.

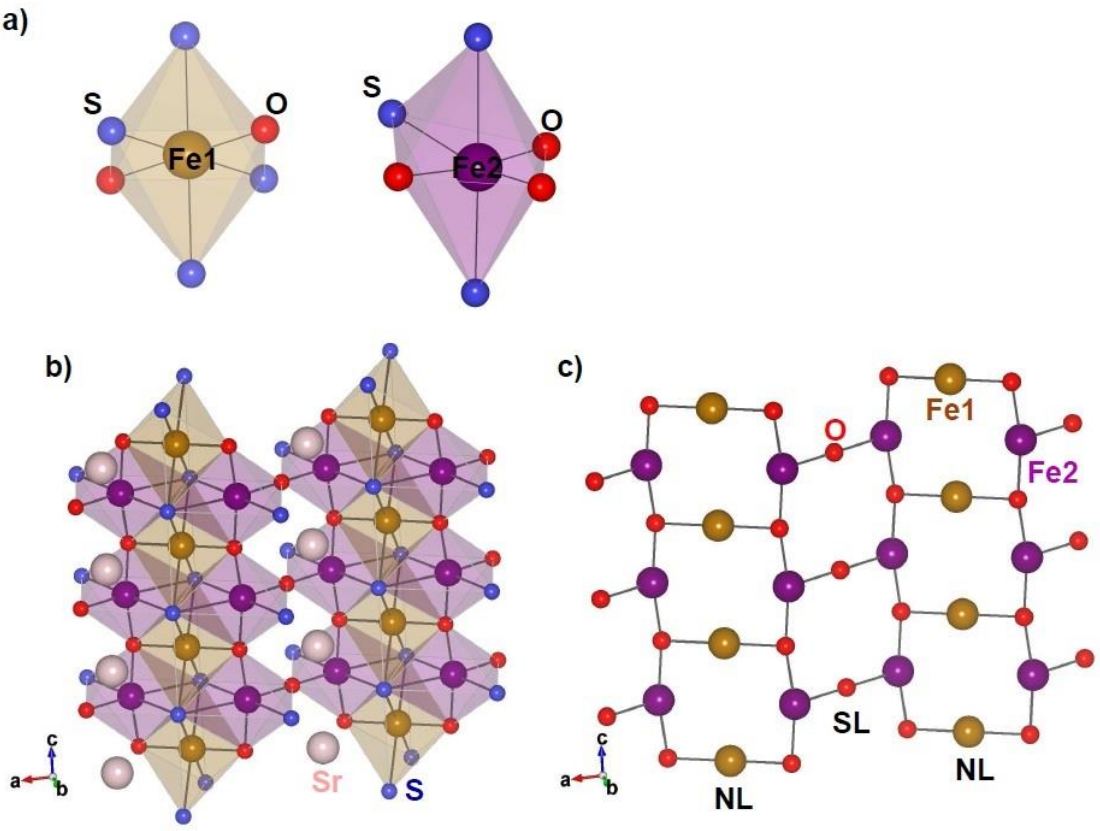

FIG 1. Crystal structure of $Sr_2Fe_3S2O_3$. (a) The basic magnetic units $Fe1S_4O_2$ and $Fe2S_3O_3$. (b) The 3-D structure formed by the legs of the ladder and Sr^{2+} ions sitting in the voids and channels. The brown, magenta, red, blue and light pink colored balls rep- resent Fe1, Fe2, O, S and Sr atoms respectively. (c) The hybrid spin ladder structure of $Sr_2Fe_3S_2O_3$.

2. Crystal Structure

$Sr_2Fe_3S_2O_3$occurs in orthorhombic symmetry space group *Pbam* (No. 55) with two formula unit per unit cell. The lattice parameters for $Sr_2Fe_3S_2O_3$ are *a*=7.7067Å, *b*=9.9098 Å, *c*=3.9545 Å.The basic magnetic units in the structure are formed two inequivalent Fe atoms, Fe1 and Fe2, sitting within distorted octahedra. The Fe1 distorted octaherda is constructed by four S-atoms and two O-atoms whereas Fe2 distorted octaherda is constructed by three S-atoms and three O-atoms, as shown in Fig.1(a).The Fe1-O and Fe1-S bond-lengths are 2.00 Å and 2.65 Å whereas Fe2-O and Fe2-S bond-lengths range from 1.98 to 2.83 Å with an average value of 2.39 Å. The distorted $Fe2S_3O_3$ octaherda share common corner and form the leg of the ladder along c-axis and also share their common edge and common corner and form the rung of theladderintheab- plane.The distorted $Fe1S_4O_2$ octaherda share common edge and form a chain a long *c*-axis and placed in between legs of the $Fe2S_3O_3$ octahedra and form necklace ladder (NL) along *c*-axis. Sr ions occupying the voids and channels in the Fe_1-Fe_2-S-O network give rise to cohesion in the structure, as shown in Fig.1(b).The hybrid spin ladder structure of $Sr_2Fe_3S_2O_3$ is shown in Fig.1(c).

3. Electronic Structure

In order to gain microscopic understanding of $Sr_2Fe_3S2O_3$ we carried out first principles density functional theory (DFT) [21] calculations within the generalized gradient approximation (GGA) [22] for the exchange-correlation functional. Calculations have been carried out in the plane wave basis as implemented within Vienna Ab initio Simulation Package (VASP) [23] as well as in muffin tin orbital (MTO) based linear MTO (LMTO) [24] basis sets. For LMTO self-consistent electronic structure calculation, the

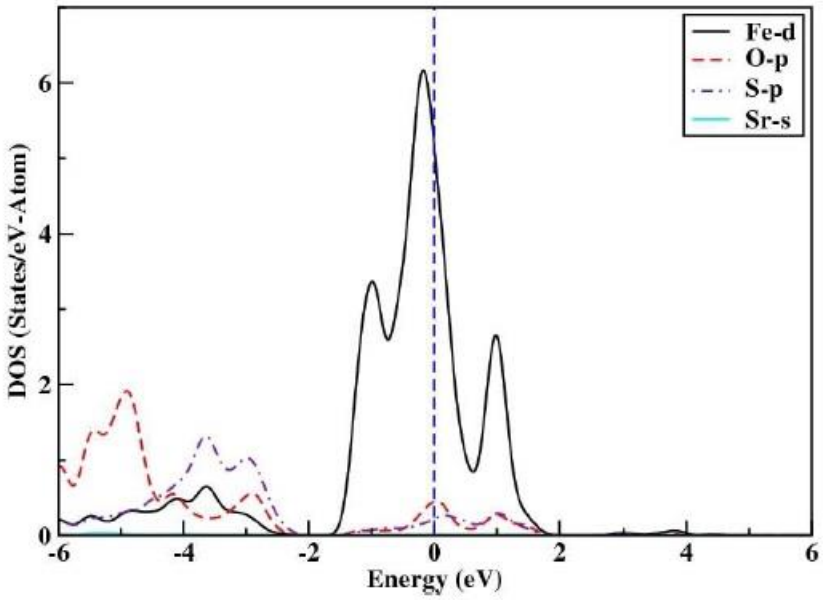

FIG 2. Non Spin polarized DOS of $Sr_2Fe_3S_2O_3$. The energy axis is plotted with respect to GGA Fermi energy.

basis set con-sisted of Sr *sd*, Fe *spd*, S *sp* and O *sp*. Seven different classes of empty spheres were used to space fill the system. The self-consistency was achieved by using 24 k-points in the irreducible Brillouin zone. The energetically accurate plane-wave basis set calculations have been employed to calculate the total energy of different spin configurations to derive the magnetic exchanges from the total-energy

method. For the self-consistent field calculations in the plane-wave basis, energy cutoff of 450 eV, and 4×4×2 Monkhorst-Pack *k*-points mesh were found to provide a good convergence of the total energy (E = 10−5 eV). The consistency between the calculations in the MTO and plane wave basis sets has been checked in terms of band structure, density of states, and magnetic moments, etc. The exchange correlation functional for the self-consistent calculations was chosen to be that of generalized gradient approximation (GGA) implemented following the Perdew-Burke-Ernzerhof prescription [22]. In the total energy calculations, the missing correlation energy at Fe sites beyond GGA calculations with supplemented Hubbard U (GGA + U) [25] were carried out, with a choice of U = 6 eV. We consider a 2×1×2 supercell for $Sr_2Fe_3S_2O_3$. We further consider 4x4x4 Monkhorst-Pack k-point mesh for the total energy calculations of various different spin configurations of $Sr_2Fe_3S_2O_3$.

3.1 Non-spin polarized density of states

Calculated density of states, projected onto Fe *d*, O *p*, S *p* and Sr *s*, as obtained within non-spin-polarized scheme of calculation for $Sr_2Fe_3S_2O_3$ is shown in Fig.2. The octahedra environment of S and oxygen atoms surrounding Fe, results into Fe-*d* state at Fermi level pronouncedly mixed with O-*p* states. We thus conclude that Fe-*d* states are primarily responsible for the electronic and magnetic behaviour of $Sr_2Fe_3S_2O_3$.

3.2 Spin polarized density of states

The corresponding spin-polarized density of states, obtained in a self-consistent spin polarized DFT calculation, projected onto Fe-*d*, O-*p*, S-*p* and Sr-*s* states, are shown in Fig.3. It is found that Fe *d*-states are completely filled in the majority spin channel and one low lying d state is filled in the minority spin channel, suggesting the nominal Fe^{2+} or d^6 valence state of Fe. The O-*p* state is found to be mostly occupied suggesting the nominal O^{2-} valence states. The oxidation state of Sr and S atoms are +2 and -2 respectively. The O-*p* state shows finite, non-zero hybridization with Fe-*d* states close to Fermi energy, which contributes to the super-exchange path of magnetic interaction between two Fe sites. The calculated magnetic moment at different sites is shown in Table 1. The total magnetic moment is $12\mu_B$ per formula unit.

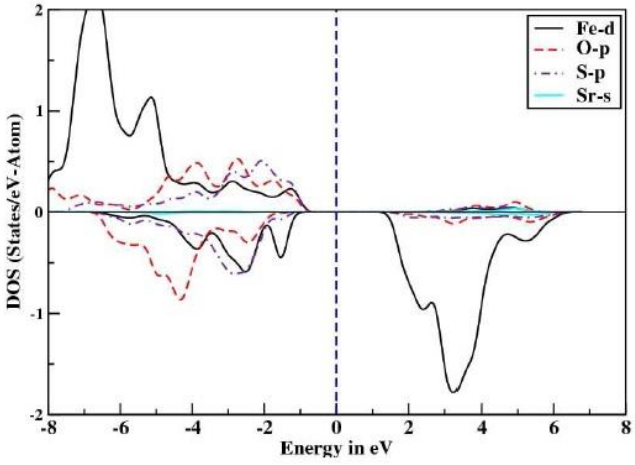

FIG 3. Spin polarized DOS of $Sr_2Fe_3S_2O_3$. Zero energy is set at the GGA Fermi energy. The states in majority and minority spin channels are shown as positive and negative values.

Table 1. The calculated magnetic moments at different atomic sites of $Sr_2Fe_3S_2O_3$.

Atom	Magnetic Moment in μ_B
Fe1	3.748
Fe2	3.778
O1	0.062
O2	0.104
Sr	0.005
S	0.088

4. Magnetic Exchanges

By performing a total energy calculation of different spin configurations of Fe atoms in $Sr_2Fe_3S_2O_3$ we estimated the various Fe-Fe magnetic exchange interactions present in the system. We constructed a supercell of dimension 2×1×2 to calculate the magnetic exchange interactions in $Sr_2Fe_3S_2O_3$, giving rise 24 Fe atoms in the unit cell. Solutions of the calculated GGA+U energies of different spin configurations to the above defined Heisenberg model gave the estimated J values. The different spin configurations of $Sr_2Fe_3S_2O_3$ is given in the Table 3.

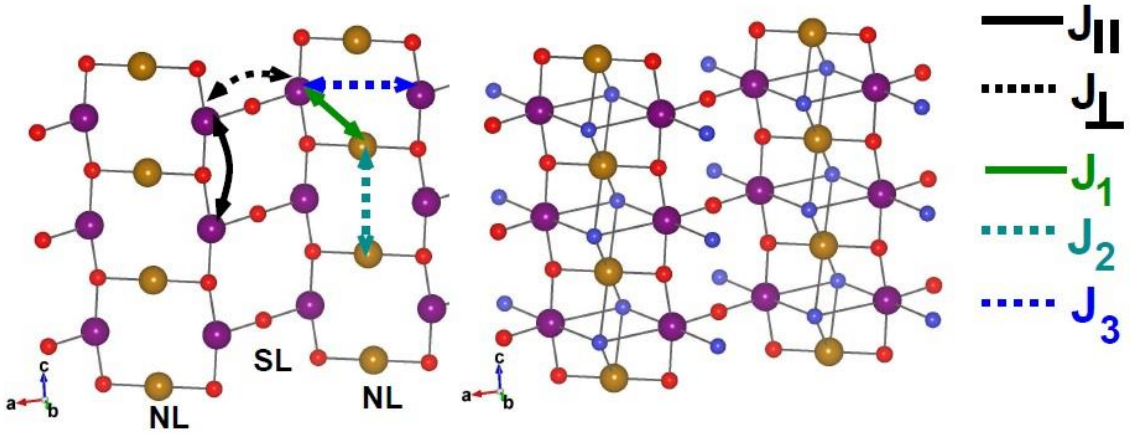

FIG 4. Interaction pathways for dominant Fe-Fe exchange interactions in $Sr_2Fe_3S_2O_3$. The superexchange paths via the O/S atoms are shown in the right panel.

Table 2. The paths and values of dominant magnetic exchange interactions in $Sr_2Fe_3S_2O_3$.

Exchange Interaction	Path	bond-angle	bond-distance	Value in K
$J_{\parallel}$	Fe2-O-Fe2	168.5°	3.95 Å	28
$J_{\perp}$	Fe2-O-Fe2	180°	4.12 Å	38
J_1	Fe1-O-Fe2	95°	2.94 Å	-18
	Fe1-O-Fe2	65°	3.95 Å	
J_2	Fe1-S-Fe1	96.4°	4.40 Å	-6
J_3	Fe2-S-Fe2	101.9°	3.95 Å	-2

The path of the dominant magnetic exchange interactions are shown in Fig.4. We see that the magnetic interaction along the legs of the SL and NL, $J_{\parallel}$ is mediated by Fe2 *d*-O *p*-Fe2 *d* super-exchange path where the Fe2-O-Fe2 bond angle is 168.5°. The magnetic interaction along the rungs of the SL, $J_{\perp}$ is mediated by Fe2 *d*-O *p*-Fe2 *d* super-exchange path where the Fe2-O-Fe2 bond angle is 180°. The magnetic interaction, J_1 is mediated by Fe1 *d*-O *p*-F2 dand Fe1 *d*-S *p*-F2 super-exchange paths where Fe1-O-F2 and Fe1-S-F2 bond-angles are 95° and 65° respectively whereas J_2 and J_3 are mediated by Fe1 *d*-S *p*-Fe1 d and Fe2 *d*-S *p*-Fe2 *d* super-exchange paths where Fe1-S-Fe1 and Fe2-S-F2 bond-angles are 96.4° and 101.9° respectively. The estimated values of dominant magnetic exchange interactions, $J_{\parallel}$, $J_{\perp}$, J_1, J_2 and J_3, between Fe-Fe sites of $Sr_2Fe_3S_2O_3$ is given in the Table 2. The positive (negative) sign of the magnetic exchange interactions indicates that the corresponding exchange interaction is antiferromagnetic (ferromagnetic) in nature.

Table 2. Magnetic configuration of the Fe ions in the supercell for the states used to determine the magnetic interactions of $Sr_2Fe_3S_2O_3$.The last column gives the relative GGA+U energies in meV.

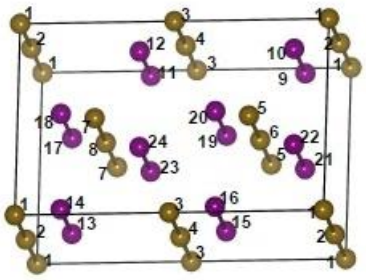

Exchange Interaction	1	2	3-4	5	6-8	9	10-14	15	16-19	20	21	22	23-24	$\triangle E$ (meV)
FM	+	+	+	+	+	+	+	+	+	+	+	+	+	0
AFM1	+	+	+	+	+	+	+	+	+	+	-	+	+	124.48746
AFM2	+	+	+	+	+	+	+	+	+	+	-	-	+	170.41707
AFM3	+	+	+	-	+	-	+	-	+	+	+	+	+	196.00185
AFM4	+	+	+	-	+	+	+	+	+	-	+	+	+	101.04639
AFM5	-	-	+	+	+	+	+	+	+	+	+	+	+	126.09443

5. Conclusion

In summary, using first-principles calculations, we have studied the electronic properties of $Sr_2Fe_3S_2O_3$.We have analysed the computed electronic structure of $Sr_2Fe_3S_2O_3$ using LMTO and VASP which provided the magnetic exchange interactions between Fe^{2+} ions. The strongest interactions, $J_{\parallel}$ and $J_{\perp}$ are AFM in nature whereas J_1 is FM. The J_2 and J_3 are order of magnitude smaller and FM in nature. Therefore, from the estimates of magnetic exchange interaction, we conclude that the system $Sr_2Fe_3S_2O_3$ is 2-D AFM spin S=2 ladder which is the origin of long range AFM order and spin gapless system.

REFERENCES

[1] D. Schmidiger, K. Yu. Povarov, S. Galeski, N. Reynolds, R. Bewley, T. Guidi, J. Ollivier and A. Zheludev, Phys. Rev. Lett. 116, 257203 (2016).
[2] M. Wang, M. Yi, S. Jin, H. Jiang, Y. Song, H. Luo, A.D. Christianson, C. de la Cruz, E.Bourret-Courchesne, D.-X. Yao, D. H. Lee, and R. J. Birgeneau, Phys. Rev. B 94, 041111(R) (2016).
[3] K. Yonaga and N. Shibata, J. Phys. Soc. Jpn. 84, 094706 (2015).
[4] I. Kimchi and A. Vishwanath, Phys. Rev. B 89, 014414 (2014).
[5] E.A. Zvereva, M.A. Evstigneeva, V.B. Nalbandyan, O.A. Savelieva, S.A. Ibragimov, O. S. Volkova, L.I. Medvedeva, A.N. Vasiliev, R. Klingeler and B. Buchner, Dalton Trans., 41, 572 (2012).
[6] S.-Y. Zhang, W.-B. Guo, M. Yang, Y.-Y. Tang, M.-Y. Cui, N.-N. Wang and Z.-Z. He, Dalton Trans., 44, 20562 (2015).
[7] H. Bethe, Z. Phys. 71, 205 (1931).
[8] E. Dagotto, and T. M. Rice, Science 271, 618 (1996).
[9] F. D. M. Haldane, Phys. Rev. Lett. 50, 1153 (1983).
[10] Y. Sasago, M. Hase, K. Uchinokura, M. Tokunaga, and N. Miura, Phys. Rev. B 52, 3533 (1995).
[11] M. Nishi, O. Fujita, and J. Akimitsu, Phys. Rev. B 50, 6508 (1994).
[12] R. M. Morra, W. J. L. Buyers, R. L. Armstrong, and K. Hirakawa, Phys. Rev. B 38, 543 (1988).
[13] M. Azuma, Z. Hiroi, M. Takano, K. Ishida, and Y. Kitaoka, Phys. Rev. Lett. 73, 3463 (1994).
[14] M. Uehara, T. Nagata, J. Akimitsu, H. Takahashi, N. Mori, K. Kinoshita, J. Phys. Soc. Jpn. 65, 2764 (1996).
[15] C. Mennerich, H. H. Klauss, M. Broekelmann, F. J. Litterst, C. Golze, R. Klingeler, V. Kataev, B. Bchner, S. N. Grossjohann, W. Brenig, M. Goiran, H. Rakoto, J. M. Broto, O. Kataeva, D. J. Price, Phys. Rev. B 73, 174415 (2006).
[16] K. T. Lai, M. Valldor, Sci. Rep 7, 43767 (2017).
[17] K. T. Lai, P. Adler, Y. Prots, Z. Hu, C. Y. Kuo, T. W. Pi and M. Valldor, Inorg. Chem. 56, 12606 (2017).
[18] M. Valldor, O. Heyer, A. C. Komarek, A. Senyshyn, M. Braden, T. Lorenz, Phys. Rev. B 83, 024418 (2011).
[19] S. Huh, Y. Ports, P. Adler, L. H. Tjeng and M. Valldor, Eur. J. Inorg. Chem, 2982 (2015).
[20] H Guo, M.T. Fernndez-Daz, A. C. Komarek, S. Huh, P. Adler and M. Valldor, Eur. J. Ionrg. Chem, 2017, 3829 (2017).
[21] W. Kohn and L.J. Sham, Phys. Rev. A 140, 1133 (1965).
[22] J.P. Perdew, K. Burke and M. Ernzerhof, Phys. Rev. Lett. 77, 3865 (1996).
[23] G. Kresse and J. Furthmuller, Phys. Rev. B 54, 11169 (1996).
[24] O.K. Andersen and O. Jepsen, Phys. Rev. Lett. 53, 2571 (1984).
[25] A.W. Sandvik, Phys. Rev. B 59, R14167 (1999).